

X-RAY DIFFRACTION, MOSSBAUER SPECTROSCOPIC AND ELECTRON MICROSCOPIC STUDY OF TIN "TITANATES" CATALYSTS USED FOR COPROCESSING MIXTURES OF COALS AND HEAVY OILS

Georges Dénès^{(a)1} and Jacques Monnier^(b)

- (a) Department of Chemistry and Laboratories for Inorganic Materials, Laboratory of Solid State Chemistry and Mössbauer Spectroscopy, CONCORDIA UNIVERSITY, 1455 West, de Maisonneuve Boulevard, Montréal, Québec, CANADA, H3G 1M8.
- (b) Energy Research Laboratories, CANMET, Energy, Mines, and Resources Canada, 555, Booth Street, Ottawa, Ontario, CANADA, K1A 0G1.

ABSTRACT

Tin "titanate" catalysts were prepared by ion exchange of sodium hydrous "titanate" $\text{NaTi}_2\text{O}_5\text{H}$ support in aqueous solutions of $\text{SnCl}_2 \cdot 2\text{H}_2\text{O}$, and tested as catalysts for coprocessing of subbituminous coals and heavy oils. The catalysts were characterized at each stage of preparation and use, i.e. before and after ionic exchange, after calcination and after use, using X-ray powder diffraction, ^{119}Sn Mössbauer spectroscopy and scanning electron microscopy. The samples are microcrystalline (30 - 300 Å particle diameter). Most of the tin is in the stannic form. The SnO_2 and TiO_2 polymorphs (rutile, anatase) present in the catalysts are stable during coprocessing. A $\text{Ti}_{1-x}\text{Sn}_x\text{O}_2$ rutile-type solid solution, found in some calcined catalysts, decomposes during coprocessing, with reduction of tin(IV) to tin(II) followed by sulfidation to SnS . This decomposition also leads to formation of TiO_2 anatase.

INTRODUCTION

The large deposits of coal and heavy oil in Western Canada have prompted extensive research on coprocessing at CANMET (1-6). Hydrogenation of coal in the presence of bitumen or heavy oil of petroleum origin yields better conversions and higher quality liquids if catalysts are added to the liquid slurry (7). Recently, the Sandia National Laboratories of the US Department of Energy developed new catalyst supports for coal hydrogenation utilizing metal-exchanged hydrous titanates (8,9).

As interesting results have been obtained using tin catalysts for hydroliquefaction of coal (10-13), new tin catalysts on hydrous "titanate"² supports were prepared and tested at CANMET for coprocessing of heavy oil and coal (5). The present study reports the characterization of the catalysts by electron microscopy, X-ray powder diffraction and ^{119}Sn Mössbauer spectroscopy (15). The structure and texture of the catalysts are discussed as a function of the method of preparation, and their effect on the catalysts behavior is examined.

- 1 Author to whom all correspondence should be addressed.
- 2 Although no structural data suggest that discrete titanate ions are present in the catalysts, we use the name "titanates", as do Dosch, Stephens, and Stohl (8,9). The name "titanates" for these type of compounds is also used in well known inorganic chemistry textbooks (14).

EXPERIMENTAL SECTION

Preparation of the Catalysts

Metal-exchanged hydrous "titanates" (MEHT) were prepared according to Dosch, Stephens, and Stohl (8,9). Reaction of titanium(IV) 2-propoxide, $Ti[OCH(CH_3)_2]_4$ with a solution of sodium hydroxide in methanol produces a soluble intermediate, which yields sodium hydrous "titanate" precipitate, $NaTi_2O_5H$, upon addition of a mixture of 10 wt % water in acetone. The precipitate is washed with water and acetone, and then dried under vacuum, yielding hydrous titanate support, in the form of a white fluffy powder. Then, the support is loaded with tin in an aqueous solution of stannous chloride dihydrate, $SnCl_2 \cdot 2H_2O$, washed with water and acetone and dried under vacuum overnight. Before hydroprocessing tests, the titanate catalysts are calcined in air at 400 °C for 2 hours. Analytical results for the metals, obtained by neutron activation, are shown in TABLE I. The samples contain much more titanium than tin or sodium. The ratio of ionic exchange of Na by Sn is 70 % for MB-586 and 46 % for MB-599.

TABLE I
Metal Content of the Catalysts

Catalyst ^a		Weight %			Atomic Ratios		
		Ti	Sn	Na	Ti/Sn	Na/Sn	Na/Ti
MB-586	nc	41.88	11.44	-	9.10	-	-
	c	43.20	12.70	1.08	8.43	0.44	0.05
	u	-	1.56	-	-	-	-
MB-599	nc	-	-	-	-	-	-
	c	36.50	16.80	3.86	5.38	1.19	0.22
	u	-	2.64	-	-	-	-

a: nc = non-calcined, c = calcined, u = used.

Characterization Techniques

The texture of the catalysts and the particles shape and size were studied by scanning electron microscopy (SEM), which was performed using a Hitachi S-520 instrument with the filament energized at 15 kV. The samples were dried at 120 °C overnight to remove adsorbed water, stored in a dessicator and then gold coated.

X-ray powder diffraction (XRD), performed on a Picker X-ray diffractometer/X-ray fluorescence spectrometer dual instrument, using the Ni-filtered K_{α} radiation of Cu ($\lambda_{K_{\alpha} Cu} = 1.54178 \text{ \AA}$), provided information on the crystalline phases present in the catalyst, namely their identification and crystalline form, and the crystallite size.

Identification of the tin species and the degree of oxidation of tin in the catalysts were obtained by Mössbauer spectroscopy, using the 8.58 % natural abundance of the ^{119}Sn probe. The 23.875 keV Mössbauer γ -ray was obtained using a 15 mCi $Ca^{119m}SnO_3$ source purchased from Amersham. A 0.1 mm thick Pd foil was used to filter the 25.04 and 25.27 keV X-ray lines. The detector was a Harshaw Na(Tl)I scintillation counter operating at 900 V. Based on the analytical data of TABLE I, the appropriate amount of sample containing 10 mg $Sn.cm^{-2}$ were enclosed in a teflon holder with a thin window and tight fitting cap. Both source and absorber (sample) were maintained at ambient temperature for the measurements. The Doppler velocity was provided by an Elscint driving system, including a MVT-4 velocity

transducer, a MFG-N-5 function generator and a MDF-N-5 driver generator, located on a vibration-free table, and operating in the triangular mode in the velocity range -8.5 mm.s^{-1} to $+8.5 \text{ mm.s}^{-1}$. The signal was fed to a Tracor Northern 7200 multichannel analyzer operating in the multiscaling mode. After accumulation of 500,000 to 1,000,000 counts per channel, data acquisition was stopped and the data were stored on a diskette. The Doppler velocity was calibrated using CaSnO_8 and $\alpha\text{-SnF}_2$ standard absorbers. Computer fitting was performed on a CDC Cyber 835 main-frame computer using GMFF5 (16), a revised version of the General Mössbauer-Fitting Program (GMFP) of Ruebenbauer and Birchall (17). All chemical isomer shifts are referenced relative to CaSnO_8 at room temperature as zero shift.

RESULTS AND DISCUSSION

Scanning Electron Microscopy

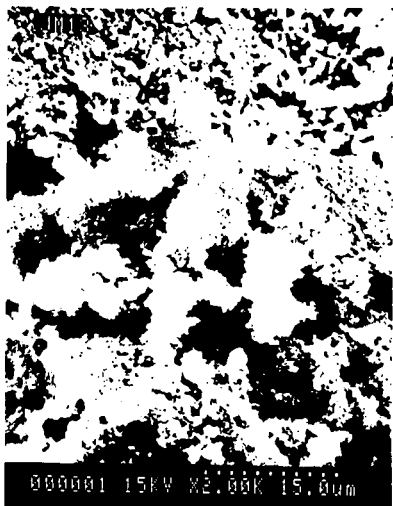
FIGURE 1 shows SEM micrographs of the hydrous titanate support (FIGURE 1a), the MB-586 catalyst before (FIGURE 1b) and after calcination (FIGURE 1c), and of MB-599 before calcination (FIGURE 1d). The support is a fine powder, non-agglomerated with particle diameters up to $2 \mu\text{m}$. Further magnification shows that the particles have no internal structure, and therefore are probably amorphous.

After ion-exchange (FIGURE 1b), a significant change has taken place as large blocks ($10 - 50 \mu\text{m}$ edge) with no particular geometrical shape are observed, together with the powder. However, magnification of such a block to 8000X reveals that it is made of loosely bound powdered particles, which again have no internal structure. After calcination (FIGURE 1c), similar types of large blocks are observed, but these are still mixed with powder and show no smaller scale structure. The loosely bound powder inside these blocks are identical to those observed before calcination, and indicate that no sintering took place. FIGURE 1d reveals that the situation is the same for the MB-599 catalyst. Scanning electron microscopy shows that all catalysts have a low degree of ordering, at all steps of preparation, with little texture. This indicates that most likely they are amorphous or microcrystalline.

X-Ray Powder Diffraction

The X-ray diffraction results for the two catalysts at various stages of preparation and use are given in FIGURES 2 and 3. FIGURE 2a shows the hydrous titanate support before ion exchange is totally amorphous. After ion-exchange (FIGURE 2b), a low degree of ordering is observed, in the MB-586 catalyst, in the form of weak, very broad bumps on the background, indicating the presence of microcrystallinity. Calcination results in significant crystallite growth, giving identifiable Bragg peaks for TiO_2 in the anatase and rutile forms and SnO_2 rutile. Little change is observed after the catalyst has been used in the coprocessing reaction, except that a few extra weak peaks indicate the formation of a small quantity of SnS and maybe some $\beta\text{-Sn}$.

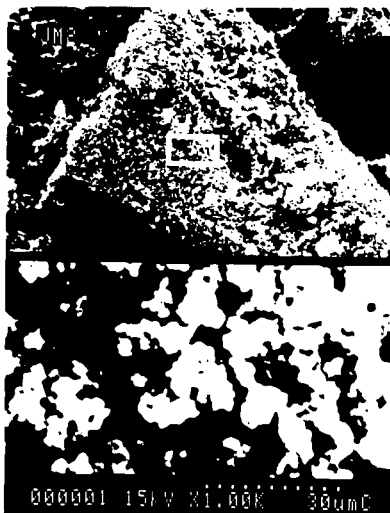
For the MB-599 catalyst (FIGURE 3), the non-calcined catalyst after ionic exchange (FIGURE 3b) is also microcrystalline. Contrary to MB-586, the powder pattern of calcined MB-599 (FIGURE 3c) contains only a few very broad peaks; however, no TiO_2 anatase, TiO_2 rutile or SnO_2 rutile seem to be present. Instead, a broad peak is observed between the positions that would be occupied by any (hkl) peak of TiO_2 rutile and the same (hkl) peak of SnO_2 rutile. This is indicative of the formation of a rutile-type $\text{Ti}_{1-x}\text{Sn}_x\text{O}_2$ solid solution with unit-cell parameters intermediate between those of TiO_2 and SnO_2 (TABLE II).



a: NaTi₃O₅H support: SEM micrograph before cationic exchange, magnification= 5,000.



b: MB-586 catalyst before calcination: SEM micrograph at magnifications of 800 (top) and 8,000 (bottom).



c: MB-586 catalyst after calcination: SEM micrograph at magnifications of 1,000 (top) and 10,000 (bottom).



d: MB-599 catalyst before calcination: SEM micrograph at magnifications of 800 (top) and 8,000 (bottom).

Figure 1

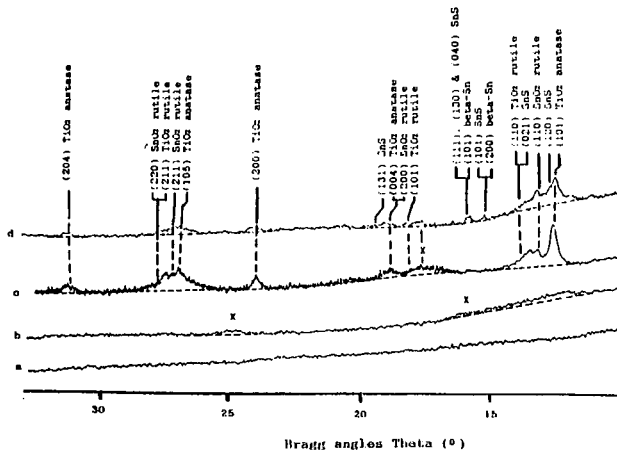


Figure 2: X-ray powder pattern (K Cu) of MB-586;
a: support
b: non-calcined ion-exchanged catalyst
c: calcined catalyst
d: used catalyst
X: unidentified peaks

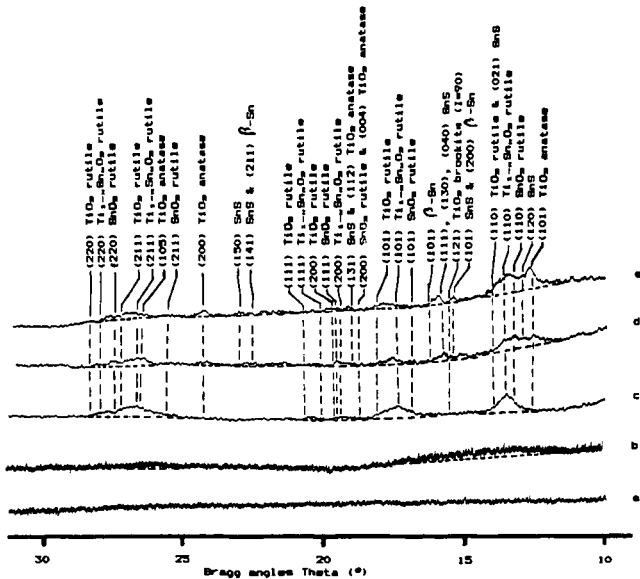


Figure 3: X-ray powder pattern (K Cu) of MB-589;
a: support
b: non-calcined ion-exchanged catalyst
c: calcined catalyst
d: used calcined catalyst
e: used non-calcined catalyst

TABLE II
Unit-Cell Parameters of TiO_2 , $Ti_{1-x}Sn_xO_2$, and SnO_2 Rutile-Type

Unit-cell parameters	TiO_2	$Ti_{1-x}Sn_xO_2$	SnO_2
a (Å)	4.594	4.643	4.738
c (Å)	2.958	3.100	3.188
V (Å ³)	62.43	66.83	71.51

Contrary to MB-586, a drastic change takes place in MB-599 upon use (FIGURE 3d and 3e), as a mixture of TiO_2 anatase, TiO_2 rutile, SnO_2 rutile, SnS , and possibly β - Sn , is observed in addition to some unreacted $Ti_{1-x}Sn_xO_2$ solid solution. The details of the changes for the first group of peaks are given on FIGURE 4.

The MB-586 and MB-599 catalysts were prepared following the same procedure, except that, for MB-599, the sodium hydroxide solution was kept below 0 °C to minimize temperature rise during addition of titanium(IV) 2-propoxide, whereas for MB-586, this NaOH solution was not cooled before preparation of the soluble titanium intermediate. This difference in experimental procedure, not brought up in the literature, must be at the origin of the difference in the nature of the solid catalysts. It is most likely that additional intermediate species, precursors of TiO_2 anatase, are formed upon hydrolysis of titanium(IV)-2-propoxide at room temperature.

The catalyst are microcrystalline at all stages, even after calcination and use, as shown by the large linewidth of the Bragg peaks. Below 1000 Å particle diameter, line broadening occurs, and below ca. 50 Å, the peaks are so broad they cannot be distinguished from the background. The average particle size of each phase was estimated by using the Scherrer's formula (18), corrected for instrumental broadening with Warren's method (18). The results are given in TABLE III.

TABLE III
Average Particle Size of Catalysts as Determined by Scherrer's Method from the Broadening of the Bragg Peaks

Catalysts ^a	$\theta(K_{\alpha}Cu)$ (°)	B_M (°) ^b	B_S (°) ^b	B (°) ^b	t(Å) ^b	Phase
Support	*	*	*	*	< 50	microcrystalline
MB-586 nc	#	#	#	#	50-100	TiO_2 microcryst. SnO_2 microcryst.
MB-586 c	12.70	0.32	0.17	0.27	300	TiO_2 anatase
MB-586 u	12.70	0.52	0.18	0.49	170	TiO_2 anatase
MB-599 nc	#	#	#	#	50-100	TiO_2 microcryst. SnO_2 microcryst.
MB-599 c	13.58 17.40	0.70 1.05	0.17 0.17	0.68 1.04	120 80	$Ti_{1-x}Sn_xO_2$ rutile $Ti_{1-x}Sn_xO_2$ rutile
MB-599 u-c	17.60	0.80	0.17	0.78	107	$Ti_{1-x}Sn_xO_2$ rutile
MB-599 u-nc	12.64 17.60	0.30 0.50	0.17 0.17	0.25 0.47	330 177	TiO_2 anatase $Ti_{1-x}Sn_xO_2$ rutile

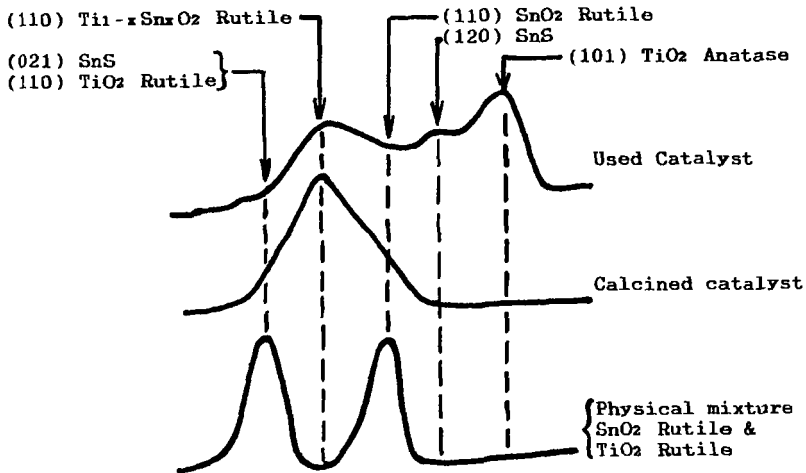


Figure 4: Comparison of the first Bragg peak of $Ti_{1-x}Sn_xO_2$ Rutile type solid solution in MB-599 calcined catalyst with a physical mixture of rutile type SnO_2 and TiO_2 and with the used catalyst.

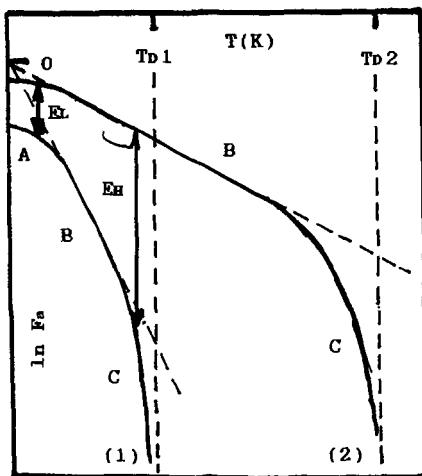


Figure 5: Evolution of the recoil-free fraction with temperature as a function of lattice strength

- A= Zero point motion
- B= Harmonic thermal vibrations
- C= Anharmonic thermal vibrations
- EL= Low temperature difference
- EH= High temperature difference
- f_a = Absorber recoil-free fraction
- T_{d1} , T_{d2} = Debye temperatures
- (1)= Soft lattice
- (2)= Hard lattice

- a: nc = non-calcined, c = calcined, u = used, u-c = used calcined catalyst, u-nc = used non-calcined catalyst.
- b: Scherrer's formula: $t = (0.9\lambda) / (B \cdot \cos\theta)$ with t (Å) = average particle size, B (°) = broadening at half-height due to small particles, λ (Å) = wavelength, θ (°) = Bragg angle.
- * No Bragg peak observed.
- # Very broad peak, cannot be measured.

X-ray diffraction results corroborate the information obtained from the SEM photographs, i.e. all samples are microcrystalline. It is not surprising that the particles of $1-2 \mu\text{m}$ diameter observed by SEM appear to have no internal structure. Indeed, each of them is made of about 10^{10} much smaller particles (diameter ca. 1000 times smaller) randomly distributed relative to one another. The support gives no Bragg peak at all, and therefore is amorphous or microcrystalline with particle diameter below 50 Å. The non-calcined ion-exchanged catalysts shows very broad features barely distinguishable from the background, indicative of a particle size close to 50 Å. The rutile-type $\text{Ti}_{1-x}\text{Sn}_x\text{O}_2$ solid solution has particle dimensions of about 100 Å, while TiO_2 anatase has the largest crystallites (~ 300 Å). Some crystallite growth occur upon calcination; however, all samples are still microcrystalline. No further crystal growth was observed during the tests.

Mössbauer Spectroscopy

^{119}Sn Mössbauer spectroscopy provides a direct probing of all tin sites, regardless of the degree of crystallinity or presence of other phases. This is very important for obtaining information on the oxidation state and the coordination of the active sites of these catalysts. Furthermore, of all metal-exchanged catalysts tested in (5), i.e. Mo, Co, Pd, Sn, and Ni, only tin has a Mössbauer isotope³. The Mössbauer results for MB-586 and MB-599 are summarized in TABLE IV.

The non-calcined ion-exchanged catalysts contain minor divalent tin and a major tetravalent tin species, both coordinated with oxygen. Sn(IV) is in pseudooctahedral coordination like in SnO_2 , with various degrees of distortion relative to regular octahedral symmetry. The oxygenated ligands can be bridging oxygen, OH^- or H_2O molecules. The sample prepared at low temperature (MB-599) contains a larger proportion of Sn(II) . Upon calcination in air, all tin(II) is oxidized to tin(IV) as expected. After coprocessing test, some stannous sulfide SnS is produced, in very small quantity (1 %) for MB-586, in much larger quantity (10 - 15 %) for MB-599. No $\beta\text{-Sn}$ was observed by Mössbauer spectroscopy; therefore, if it is indeed formed, it is in very small quantities.

Mechanism of formation of TiO_2 anatase and SnS during the coprocessing reaction

The X-ray diffraction results of FIGURES 2 to 4 and the Mössbauer data presented in TABLE IV show that, during coprocessing, a profound change takes place in the solid catalyst provided it was

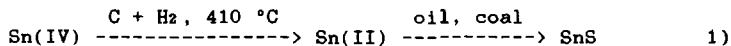
- 3 Co catalysts can be studied by ^{57}Fe Mössbauer spectroscopy; however, this requires preparing the catalyst using radioactive ^{57}Co radioisotope, thus giving rise to additional experimental complications. In addition, electron-capture decay, and the following Auger cascade, often give extra Mössbauer lines and unexpected oxidation states of Fe, making the interpretation of the spectra more difficult (19).

TABLE IV
Room Temperature ^{119}Sn Mössbauer Parameters for MB-586 and MB-599 Tin Titanate Catalysts

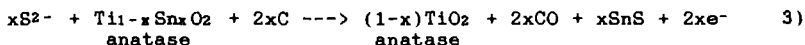
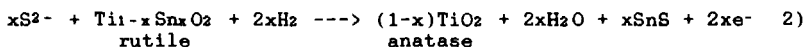
Catalysts ^a	δ (mm.s ⁻¹) ^b	Δ (mm.s ⁻¹) ^c	Oxid	Contr(%) ^e	Assignment ^f
MB-586 nc	- 0.09	0.15	+4	95	Sn/O octa sd
	3.04	1.59	+2	5	Sn(II)/O
MB-586 c	- 0.03	0.30	+4	100	Sn/O octa di
MB-586 u	- 0.03	0.40	+4	99	Sn/O octa vd
	3.16	0.98	+2	1	SnS
MB-599 nc	- 0.09	0.40	+4	75	Sn/O octa vd
	3.13	1.78	+2	25	Sn(II)/O
MB-599 c	- 0.03	0.00	+4	100	Sn/O octa ud
MB-599 u-c	- 0.03	0.00	+4	85	Sn/O octa ud
	3.22	0.86	+2	15	SnS
MB-599 u-nc	- 0.03	0.00	+4	90	Sn/O octa ud
	3.28	0.86	+2	10	SnS

- a: nc = non-calcined, c = calcined, u = used, u-c = used calcined catalyst, u-nc = used non-calcined catalyst.
b: chemical isomer shift relative to CaSnO_3 at room temperature, error bar = 0.01 mm.s⁻¹.
c: quadrupole splitting, error bar = 0.01 mm.s⁻¹.
d: oxi = tin oxidation state.
e: contr = % contribution of each tin site to the total spectrum, error bar = 1 %.
f: Sn/O octa = tetravalent tin in octahedral or pseudo-octahedral coordination of oxygen, ud = undistorted, sd = slightly distorted, di = distorted, vd = very distorted, Sn(II)/O = divalent tin coordinated by oxygen.

formed of $\text{Ti}_{1-x}\text{Sn}_x\text{O}_2$ solid solution (MB-599). The amount of solid solution is reduced while a large amount of TiO_2 anatase is formed and ca. 15 % SnS. On the other hand, if the calcined catalyst contains TiO_2 anatase and rutile and SnO_2 rutile, and no $\text{Ti}_{1-x}\text{Sn}_x\text{O}_2$ (MB-586), no significant change is observed and little SnS is formed (1 %). Obviously, there is a correlation between the simultaneous disappearance of $\text{Ti}_{1-x}\text{Sn}_x\text{O}_2$ and the appearance of TiO_2 anatase and SnS. As the reaction with calcined MB-599 gives the highest yield in SnS, reduction of tin(IV) to tin(II) by hydrogen and/or coal first takes place, followed by sulfidation of the tin(II) formed (EQUATION 1), sulfur being provided by the oils (5 wt % S) and coals (0.5 wt % S).



As formation of SnS is observed only if $\text{Ti}_{1-x}\text{Sn}_x\text{O}_2$ is present, the reactions given in EQUATIONS 2 and 3 take place at 410 °C under 3.4 MPa pressure of hydrogen.



Reactions 2 and 3 produce TiO_2 anatase and SnS and consume $Ti_{1-x}Sn_xO_2$, and therefore, account for the experimental observations. The reason the reaction works well with $Ti_{1-x}Sn_xO_2$ and not for SnO_2 rutile is probably that the SnO_2 lattice is much more stable. Indeed, the strain induced by the presence of two cations of significantly different size ($Sn(IV) = 0.83 \text{ \AA}$, $Ti(IV) = 0.735 \text{ \AA}$, in coordination number six) (20) in $Ti_{1-x}Sn_xO_2$ reduces the lattice energy and makes it more susceptible to the destabilizing power of chemical attacks.

The amount of SnS formed depends on the presence of the $Ti_{1-x}Sn_xO_2$ rutile-type solid solution, and is not favored by prior presence of tin(II) in the catalyst. The data of TABLE V show that the calcined MB-599 (0 % Sn(II)) yields 15 % SnS, while non-calcined MB-599 catalyst (25 % Sn(II)) gives 10 % SnS, i.e. less. Even in the case of the test with non-calcined MB-599, the used catalyst contains less divalent tin (10 %) than the catalyst before use (25 %), showing that direct sulfidation of tin(II) already present does not take place. To the contrary, presence of $Ti_{1-x}Sn_xO_2$ is required showing that its decomposition leads to SnS and TiO_2 anatase, according to equations 2 and/or 3.

TABLE V
Amount of SnS versus Test Conditions

Catalyst	c/nc ^a	Ts ^b	pH ₂ (psi) ^c	Tr (°C) ^d	Time ^e	% SnS
MB-586	c	RT	500	410	3h45	1
MB-599	c	< 0 °C	500	410	3h45	15
MB-599	nc	< 0 °C	500	410	3h45	10

- a: c = calcined, nc = non-calcined.
 b: Ts = temperature of preparation of support.
 c: pH₂ = pressure of hydrogen (continuous flow) in the reactor during the test.
 d: Tr = temperature of reaction for the tests.
 e: Time = time of the test reaction.

A surprising feature is the high amount of Sn(IV) in the catalysts before calcination, i.e. the large amount of divalent tin oxidized to tin(IV) during ion-exchange. TABLE V compares the relative amount of tin(II) as a function of the conditions of ion exchange.

TABLE VI
Relative amount of divalent tin in ion-exchanged non-calcined catalysts as a function of preparative conditions

Catalyst	Water Degassing	pH	Stirring Time (min)	Sn(II)/total Sn (%)
MB-586	No	2.8	60	5
MB-599	Yes	1.83	105	25
MB-585	Yes	2.4	60	10

Although one could expect that prolonged exposure to dissolved atmospheric oxygen would increase the amount of tin(IV), the above data clearly indicate that the pH of the solution is the most important factor, followed by degassing. Most likely, at low pH less hydrolysis of tin(II) occurs, which is known to favor oxidation. However, a pH lower than 1.8 cannot be used because it dissolves the sodium titanate support. Oxidation to tin(IV) during calcination could be expected.

CONCLUSION

Tin exchanged hydrous "titanates" have been prepared and characterized by some of the solid state techniques. The method of preparation, texture and structure of the catalysts, as well as the nature of the tin site, are important parameters for the understanding of their behavior during coprocessing reactions. The catalysts are microcrystalline in all stages of preparation, although significant crystallite growth of TiO_2 anatase occurs during calcination, from ca. 50 Å to 300 Å. The method of preparation of the support is critical as a room temperature reaction yields mostly TiO_2 anatase, while low temperature syntheses result in a rutile-type $\text{Ti}_{1-x}\text{Sn}_x\text{O}_2$ solid solution being formed, which easily decomposes upon reduction of tin(IV) to tin(II), producing SnS and TiO_2 anatase at coprocessing conditions. X-ray diffraction and Mössbauer spectroscopy show that no Sn(IV) or Sn(II)/Sn(IV) mixed oxidation state sulfide is formed. In addition, no titanium sulfide or sodium-containing species was detected, despite the non-negligible sodium content (TABLE I). The coal/hydrogen reducing medium reduces Sn(IV) from $\text{Ti}_{1-x}\text{Sn}_x\text{O}_2$ and not from SnO_2 , followed by sulfidation to SnS, using the natural sulfur content of coals and oils. TiO_2 anatase and rutile and SnO_2 rutile seem very stable.

The relative contribution of each tin species to the total Mössbauer spectrum, is not equal to the real amounts of these species in the samples if their recoil-free fractions are not the same, and the difference, which is a function of their Debye temperature, is temperature dependent, as shown on FIGURE 5. A variable temperature study is presently being undertaken in order to minimize the error due to recoil-free fraction difference. Calculations of equilibrium constants (21) for the reduction of oxides of Sn, Mo, Co, and Ni, at the temperature of the coprocessing reactions show that SnO_2 is more difficult to reduce in H_2 than NiO, CoO and MoO₃. If reduction of SnO_2 occurred, NiO, CoO and MoO₃ would also be reduced in the reactions of (5). As no data are available on the equilibrium constant for $\text{Ti}_{1-x}\text{Sn}_x\text{O}_2$, reduction of NiO, CoO, and MoO₃ cannot be confirmed. The detailed study of the tin catalysts, which was possible because of the ^{119}Sn Mössbauer probe, provides a model for catalysts containing other metals, which have no Mössbauer nuclide.

ACKNOWLEDGMENT

We wish to thank Prof. N. Kapoor, Ms. J. Fitzgerald, and Mrs. M. Dènès at Concordia University for technical assistance in electron microscopy and X-ray diffraction. Financial assistance from Concordia University for the purchase of the Mössbauer spectrometer and technical assistance from the Concordia University Science Technical Center are acknowledged. G.D. thanks the Natural Sciences and Engineering Research Council of Canada for a University Research Fellowship. This work was conducted under Supply and Services Canada Contract Serial Number OST85-00243.

REFERENCES

1. J.F. Kelly, S.A. Fouda, P.M. Rahimi, and M. Ikura, Proceedings of the Coal Conversion Contractors' Review Meeting, J.F. Kelly Edit.; CANMET, Energy, Mines and Resources Canada, Ottawa, Ontario, Canada, 397 (1985).
2. J. Monnier and J.F. Kriz, Ind. Eng. Chem. Prod. Res. Dev. 25, 537 (1986).
3. S.A. Fouda and J.F. Kelly, Proceedings of the 1987 International Conference on Coal Science; J.A. Moulijn et al. Eds., Elsevier Science Publishers, 387 (1987).
4. P.M. Rahimi, S.A. Fouda, and J.F. Kelly, Proceedings of the 12th EPRI Annual Fuel Science and Conversion Conference, Palo Alto, California, USA (1987).
5. J. Monnier, G. Dénès, J. Potter, and J.F. Kriz, J. Energy & Fuels 1, 332 (1987).
6. J. Monnier, C.W. Fairbridge, J.R. Brown, and J.F. Kriz, Proceedings of the 9th International Congress on Catalysis 1, 182 (1988).
7. J. Monnier and J.F. Kriz, 10th Canadian Symposium on Catalysis, Preprints, 1 (1986).
8. R.G. Dosch, H.P. Stephens, and F.V. Stohl, US Patent 4 511 455 (1985).
9. H.P. Stephens, R.G. Dosch, and F.V. Stohl, Ind. Eng. Chem. Prod. Res. Dev. 24, 15 (1985).
10. S.W. Weller, in "Catalysis IV", P. Emmett Edit., Reinhold, New York, CHAPTER 7 (1956).
11. S.J. Cochran, M. Hatswell, W. Roy Jackson, and F.P. Larskins, Fuel 61, 831 (1982).
12. M. Mizumoto, H. Yamashita, and S. Matsuda, Ind. Eng. Chem. Prod. Res. Dev. 24, 394 (1985).
13. P.S. Cook and J.D. Cashion, Fuel 65, 146 (1986).
14. F.A. Cotton and G. Wilkinson, "Advanced Inorganic Chemistry", 4th Ed., Wiley-Interscience, New York, USA, p. 695 (1980).
15. G. Dénès, "Characterization of Tin Catalysts by Mössbauer Spectroscopy", Final Report to CANMET under Supply and Services Canada Contract Serial Number OST85-00243; Department of Chemistry, Concordia University, Montréal, Québec, Canada (1987).
16. J. Monnier, G. Dénès, and R.B. Anderson, Can. J. Chem. Eng. 62, 419 (1984).
17. K. Ruebenbauer and T. Birchall, Hyperfine Interact. 7, 125 (1979).
18. B.D. Cullity, "Element of X-ray Diffraction", 2nd Ed., Addison-Wesley, Don Mills, Ontario, Canada, pp. 192, 284 (1978).
19. N.N. Greenwood and T.C. Gibb, "Mössbauer Spectroscopy", Chapman and Hall Limited, London, UK, p. 330 (1971).
20. R.D. Shannon, Acta Crystallogr. A32, 751 (1976).
21. I. Barin and O. Knacke, "Thermochemical Properties of Inorganic Substances", Springer-Verlag, West-Berlin, Germany, and New York, USA (1973).